

Research Article

Potent and Selective Inhibition of Polycythemia by the Quinoxaline JAK2 Inhibitor NVP-BSK805

Fabienne Baffert¹, Catherine H. Régnier¹, Alain De Pover¹, Carole Pissot-Soldermann², Gisele A. Tavares³, Francesca Blasco⁴, Josef Brueggen¹, Patrick Chène¹, Peter Druce³, Dirk Erdmann¹, Pascal Furet², Marc Gerspacher², Marc Lang², David Ledieu⁵, Lynda Nolan⁵, Stephan Ruetz¹, Joerg Trappe³, Eric Vangrevelinghe², Markus Wartmann¹, Lorenza Wyder¹, Francesco Hofmann¹, and Thomas Radimerski¹

Abstract

The recent discovery of an acquired activating point mutation in JAK2, substituting valine at amino acid position 617 for phenylalanine, has greatly improved our understanding of the molecular mechanism underlying chronic myeloproliferative neoplasms. Strikingly, the JAK2^{V617F} mutation is found in nearly all patients suffering from polycythemia vera and in roughly every second patient suffering from essential thrombocythemia and primary myelofibrosis. Thus, JAK2 represents a promising target for the treatment of myeloproliferative neoplasms and considerable efforts are ongoing to discover and develop inhibitors of the kinase. Here, we report potent inhibition of JAK2^{V617F} and JAK2 wild-type enzymes by a novel substituted quinoxaline, NVP-BSK805, which acts in an ATP-competitive manner. Within the JAK family, NVP-BSK805 displays more than 20-fold selectivity towards JAK2 *in vitro*, as well as excellent selectivity in broader kinase profiling. The compound blunts constitutive STAT5 phosphorylation in JAK2^{V617F}-bearing cells, with concomitant suppression of cell proliferation and induction of apoptosis. *In vivo*, NVP-BSK805 exhibited good oral bioavailability and a long half-life. The inhibitor was efficacious in suppressing leukemic cell spreading and splenomegaly in a Ba/F3 JAK2^{V617F} cell-driven mouse mechanistic model. Furthermore, NVP-BSK805 potently suppressed recombinant human erythropoietin-induced polycythemia and extramedullary erythropoiesis in mice and rats. *Mol Cancer Ther*; 9(7); 1945–55. ©2010 AACR.

Introduction

The discovery of an acquired activating point mutation in the pseudokinase domain of JAK2 in patients suffering from chronic myeloproliferative neoplasms (cMPN; refs. 1–3) has drawn a lot of attention to this kinase. For the first time, there is a molecular understanding of the underlying disease mechanism and, equally of importance, the mutated JAK2 is a druggable target for therapeutic intervention (4, 5). The JAK2 valine 617 to phenylalanine mutation is found in nearly every patient with polycythemia vera (PV) as well as in approximately every second

patient suffering from essential thrombocythemia and primary myelofibrosis (6). Interestingly, in the remainder of V617F-negative PV patients, mutations were discovered in JAK2 exon 12, also affecting the pseudokinase domain (7). In Down's syndrome-associated acute lymphoblastic leukemia, yet another JAK2-activating pseudokinase point mutation was identified, affecting arginine 683 (8, 9). Aberrant JAK2 signaling can also be brought about by mutations in receptors. For instance, W515L/K mutations in the thrombopoietin receptor account for ~5% to 10% of V617F-negative essential thrombocythemia and primary myelofibrosis cases (10, 11). Loss of negative feedback regulation as a consequence of suppressor of cytokine signaling silencing or mutation has been described in certain lymphomas (12). Furthermore, chromosomal translocations that involve the JAK2 kinase, such as the t(9;12) TEL-JAK2 fusion in rare cases of T-cell acute lymphoblastic leukemia, can also cause constitutive kinase activation (13). Thus, the patient population that is anticipated to benefit from JAK2 inhibitor treatment is fairly well defined by a series of alterations that confer dependency on JAK2 signaling. Encouragingly, clinical trials in patients suffering from cMPNs are already under way with first-generation JAK inhibitors (14).

Here, we describe the discovery of a novel substituted quinoxaline, termed NVP-BSK805, as a potent and selective ATP-competitive inhibitor of JAK2. The binding

Authors' Affiliations: ¹Disease Area Oncology, ²Global Discovery Chemistry, ³Center for Proteomic Chemistry, ⁴Metabolism and Pharmacokinetics, and ⁵Preclinical Safety Clinical Pathology, Novartis Institutes for BioMedical Research, Basel, Switzerland

Note: Supplementary material for this article is available at Molecular Cancer Therapeutics Online (<http://mct.aacrjournals.org/>).

Current address for L. Wyder: Actelion Pharmaceuticals, Ltd., Allschwil, Switzerland.

Corresponding Authors: F. Hofmann and T. Radimerski, Disease Area Oncology, Novartis Institutes for BioMedical Research, Klybeckstrasse 141, 4057 Basel, Switzerland. Phone: 41-61-696-2064; Fax: 41-61-696-3835. E-mail: francesco.hofmann@novartis.com and thomas.radimerski@novartis.com

doi: 10.1158/1535-7163.MCT-10-0053

©2010 American Association for Cancer Research.

mode was corroborated by solving the structure of the kinase-inhibitor complex. NVP-BSK805 displays more than 20-fold selectivity over the other JAK family members and more than 100-fold selectivity over a panel of kinases *in vitro*. In cells bearing JAK2^{V617F}, NVP-BSK805 potently inhibited constitutive STAT5 phosphorylation, blocked cell proliferation, and triggered apoptosis. In mechanistic animal models of JAK2^{V617F}-driven leukemic disease and rhEpo-mediated polycythemia, NVP-BSK805 displayed a long duration of action, suppressed STAT5 phosphorylation in target tissues, leukemic cell spreading and splenomegaly, while being well tolerated.

Materials and Methods

Compounds and formulations

NVP-BSK805 (free base) was synthesized internally (15). "JAK inhibitor 1" was from Calbiochem. Compounds were prepared as 10 mmol/L stock solutions in DMSO and stored at -20°C . For dosing of mice, NVP-BSK805 was freshly formulated in NMP/PEG300/Solutol HS15 (5/80/15%) and applied at 10 mL/kg by oral gavage.

Cell culture

SET-2 cells (generously provided by Prof. Hans Drexler, DSMZ, Braunschweig, Germany) and K-562 cells (American Type Culture Collection) were cultured in RPMI medium supplemented with 10% FCS, 2 mmol/L of L-glutamine, and 1% (v/v) penicillin/streptomycin. CMK cells (DSMZ) were grown in RPMI medium as described above, supplemented with 20% FCS. MB-02 cells (generously provided by Prof. Doris Morgan, Drexel University, Philadelphia, PA) were grown in RPMI medium as described above, supplemented with 10 ng/mL of granulocyte macrophage colony-stimulating factor, 10 ng/mL of stem cell factor, and 10 mmol/L of sodium pyruvate. UKE-1 cells (generously provided by Prof. Walter Fiedler, University Hospital Eppendorf, Hamburg, Germany) were cultured in Iscove's modified Dulbecco's medium with 10% FCS, 10% horse serum, 1 $\mu\text{mol/L}$ of hydrocortisone, and 1% (v/v) penicillin/streptomycin. MUTZ-8 cells (provided by Prof. Hans Drexler) were grown in 80% MEM α supplemented with 20% heat-inactivated FCS, 1% (v/v) penicillin/streptomycin, 20 ng/mL of granulocyte macrophage colony-stimulating factor, 20 ng/mL of SCF, and 20 ng/mL of IL-3.

Western blotting

Cells were extracted in lysis buffer [50 mmol/L HEPES (pH 7.4), 150 mmol/L NaCl, 25 mmol/L β -glycerophosphate, 25 mmol/L NaF, 5 mmol/L EGTA, 1 mmol/L EDTA, 15 mmol/L pyrophosphate PPI, supplemented freshly with 1% NP40, 1 \times protease inhibitor cocktail (Complete Mini, Roche), 1 mmol/L DTT, 0.2 mmol/L sodium-vanadate, and 1 mmol/L phenylmethylsulfonyl fluoride] by passing through a 1 mL syringe connected to a 23-gauge needle. Cell debris

were pelleted by centrifugation. Typically, 20 μg of protein lysates were resolved by SDS-PAGE and transferred to polyvinylidene difluoride membranes by semi-dry blotting. JAK1, JAK2, phosphorylated STAT5, PARP, and Bcl-xL antibodies were from Cell Signaling Technology. JAK3, STAT5, and TYK2 antibodies were from Santa Cruz Biotechnology. Bim and β -tubulin antibodies were from Calbiochem and Sigma, respectively. Antibodies were typically incubated overnight at 4°C followed by washes and incubation with the corresponding horseradish peroxidase-conjugated secondary antibodies. Immunoreactive bands were revealed with enhanced chemiluminescence reagents.

X-ray crystallography

Crystals were grown at 20°C using the hanging drop vapor-diffusion method. Purified JAK2-NVP-BSK805 complex (molar ratio 1:3) at 9 mg/mL in 20 mmol/L of Tris, 250 mmol/L of NaCl, 1 mmol/L of DTT (pH 8.5) was mixed with an equal volume of a reservoir solution containing 1.2 mol/L of sodium citrate, 0.1 mol/L of HEPES (pH 7.5). Plate-like crystals grew within 2 days. A cryoprotectant consisting of 30% glycerol in reservoir solution was used for flash-cooling the sample in liquid nitrogen. During data collection, the crystal was cooled at 100 K. Diffraction data were collected at the Swiss Light Source (beamline X10SA) using a Marresearch CCD detector and an incident monochromatic X-ray beam with 0.97812 \AA wavelength. Raw diffraction data were processed and scaled with the XDS/XSCALE software package. The structure was determined by molecular replacement with PHASER as implemented in CCP4 using the coordinates of JAK2 in complex with a pan-Janus kinase inhibitor (PDB code 2B7A) as a search model (16). The program REFMAC was used for structure refinement using all diffraction data between 50 and 1.8 \AA resolution, excluding 5% of the data for cross-validation. The final model converged at $R_{\text{work}} = 16.7\%$ ($R_{\text{free}} = 20.6\%$). The refined coordinates of the complex structure have been deposited in the Research Collaboratory for Structural Bioinformatics Protein Data Bank under accession code 3KRR.

Proliferation assays

The antiproliferative activity of JAK2 inhibitors was determined by incubating cells for 72 hours (96 hours for MB-02 and MUTZ-8 cells) with an 8-point concentration range of compound and cell proliferation relative to DMSO-treated cells was measured using the colorimetric WST-1 (Roche Diagnostics GmbH) cell viability readout. Of each triplicate treatment, the mean was calculated and these data were plotted in XLfit 4 (ID Business Solutions, Ltd.) to determine the half-maximal growth inhibition (GI_{50}) values.

Ba/F3 JAK2^{V617F}-luc mouse model

Individual cell clones of Ba/F3 cells stably expressing human EpoR, JAK2^{V617F}, and firefly luciferase (kindly

provided by Dr. Gang Xia, GNF, San Diego, CA) were isolated by means of limiting dilution. Individual clones were characterized *in vitro*, followed by assessment of growth *in vivo* and selection of a suitable clone (clone 8; designated Ba/F3 JAK2^{V617F}-luc cells herein). Ba/F3 JAK2^{V617F}-luc cells grown to confluency were resuspended in HBSS and kept on ice until i.v. tail vein injection (1×10^6 cells in 200 μ L total volume per animal). Luciferase-expressing leukemic cells were visualized *in vivo* with the IVIS imaging system (Xenogen Corporation). Animals were injected i.p. with a mix of ketamine (65 mg/kg), xylazine (12 mg/kg), acepromazine (2 mg/kg), and with D-luciferin (Xenogen Corporation) at a dose of 150 mg/kg. Imaging was done 15 minutes after injection of D-luciferin. Light emission was quantified with the Living Image v2.20 software package (Xenogen Corporation). Antitumor activity was expressed as % T/C (mean increase of bioluminescence of treated animals divided by the mean increase of bioluminescence of control animals multiplied by 100). All experiments were done with female severe combined immunodeficiency (SCID) beige mice 6 to 8 weeks of age obtained from Taconic Farms (CB17/GbmsTac-SCID Beige, Denmark). Animals were kept under pathogen-controlled conditions with free access to food and water. Treatments were initiated on day 5 after cell injection for efficacy studies, a day after detectable luciferase signals could be measured, or on day 9 for pharmacodynamic analysis of animals with established disease.

Mouse rhEpo-induced polycythemia model

Concomitantly with NVP-BSK805 treatment, female BALB/c mice (Charles River) received daily s.c. injections (in 100 μ L saline buffer) of 10 units of rhEpo (Cell Sciences) for 4 consecutive days. Controls were injected corresponding volumes of saline buffer. Mice were sacrificed 24 hours after the final dose and total blood, spleen, and bone marrow were taken for further analysis. Animals were 8 to 10 weeks of age at treatment start (20–25 g body weight) and were kept under optimal hygienic conditions with free access to food and water. All animal experiments were done in strict adherence to Swiss laws for animal welfare and approved by the Swiss Cantonal Veterinary Office of Basel-Stadt.

Complete blood count analysis

Blood was collected from mice and rats anesthetized with isoflurane through the posterior vena cava into EDTA-coated microtubes (BD Microtainer). Blood analyses were done on the ADVIA 120 blood analyzer (Bayer Diagnostics).

Statistical analysis

When applicable, *in vivo* results were presented as mean \pm SEM. Absolute values or log₁₀ transformed values for spleen, bioluminescence, and hematologic variables were used to make statistical comparisons between groups (one-way ANOVA followed by Dunnett's test or

ANOVA on ranks followed by Dunn's test). For multiple comparisons, Tukey or Dunn's test were done. The significance level was set at $P < 0.05$. Statistical analysis was done using SigmaStat v3.1 (Jandel Scientific).

Results

Potent and selective inhibition of JAK2 *in vitro* by a novel substituted quinoxaline

JAK2 has emerged as a promising drug target in hematologic malignancies (17). Given the indolent and chronic nature of myeloproliferative neoplasms, the ideal JAK2 inhibitor must have a favorable safety profile while displaying good selectivity for JAK2 within the JAK family to avoid unwanted immunosuppression (18, 19). The structure of the JAK2 tyrosine kinase domain in complex with a pan-JAK inhibitor tool compound (16) provided a basis for molecular modeling and drug design. Reiterative scaffold morphing of an initial lead chemotype and transfer of structure-activity relationship information yielded 2,8-diaryl-substituted quinoxalines with promising JAK2 inhibitory activity and good intrinsic JAK2 selectivity versus the other JAK family members. Successive optimization for potency, kinase and receptor panel selectivity as well as favorable absorption, distribution, metabolism, and excretion properties, resulted in NVP-BSK805 (Fig. 1A; ref. 15). NVP-BSK805 was found to potently inhibit JAK2, whereas displaying more than 20-fold selectivity towards JAK1, JAK3, and TYK2 (Table 1). NVP-BSK805 elicited half-maximal inhibition of full-length JAK2^{V617F} and JAK2 wild-type enzymes (20) at 0.5 nmol/L (Table 1). For sake of reference, these studies were also carried out with the pan-JAK inhibitor "JAK inhibitor 1" (Table 1; ref. 21). The kinase selectivity of NVP-BSK805 was assessed in an internal kinase panel. The results confirmed potent inhibition of JAK2 by NVP-BSK805, along with good selectivity towards the other three JAK family members, and indicated that the compound is also fairly selective against other kinases (Supplementary Table S1). The mode of action of NVP-BSK805 was determined by incubating the JAK2 catalytic domain with different concentrations of ATP and the inhibitor. These experiments revealed that NVP-BSK805 is an ATP-competitive inhibitor (Fig. 1B). The K_i was calculated as 0.43 ± 0.02 nmol/L. The binding mode was corroborated by solving the crystal structure of the active JAK2 protein tyrosine kinase domain (16) in complex with NVP-BSK805 at a resolution of 1.8 Å (Fig. 1C). The quinoxaline pharmacophore was found to bind deeply in the ATP-binding site, making contact with the hinge region. The polar piperidinyl-pyrazole moiety, which provides solubility at neutral pH, extends through the hydrophobic channel and is exposed to the solvent. In contrast, the difluorobenzyl-morpholine substituent reaches into the hydrophobic pocket towards the glycine loop (Fig. 1D).

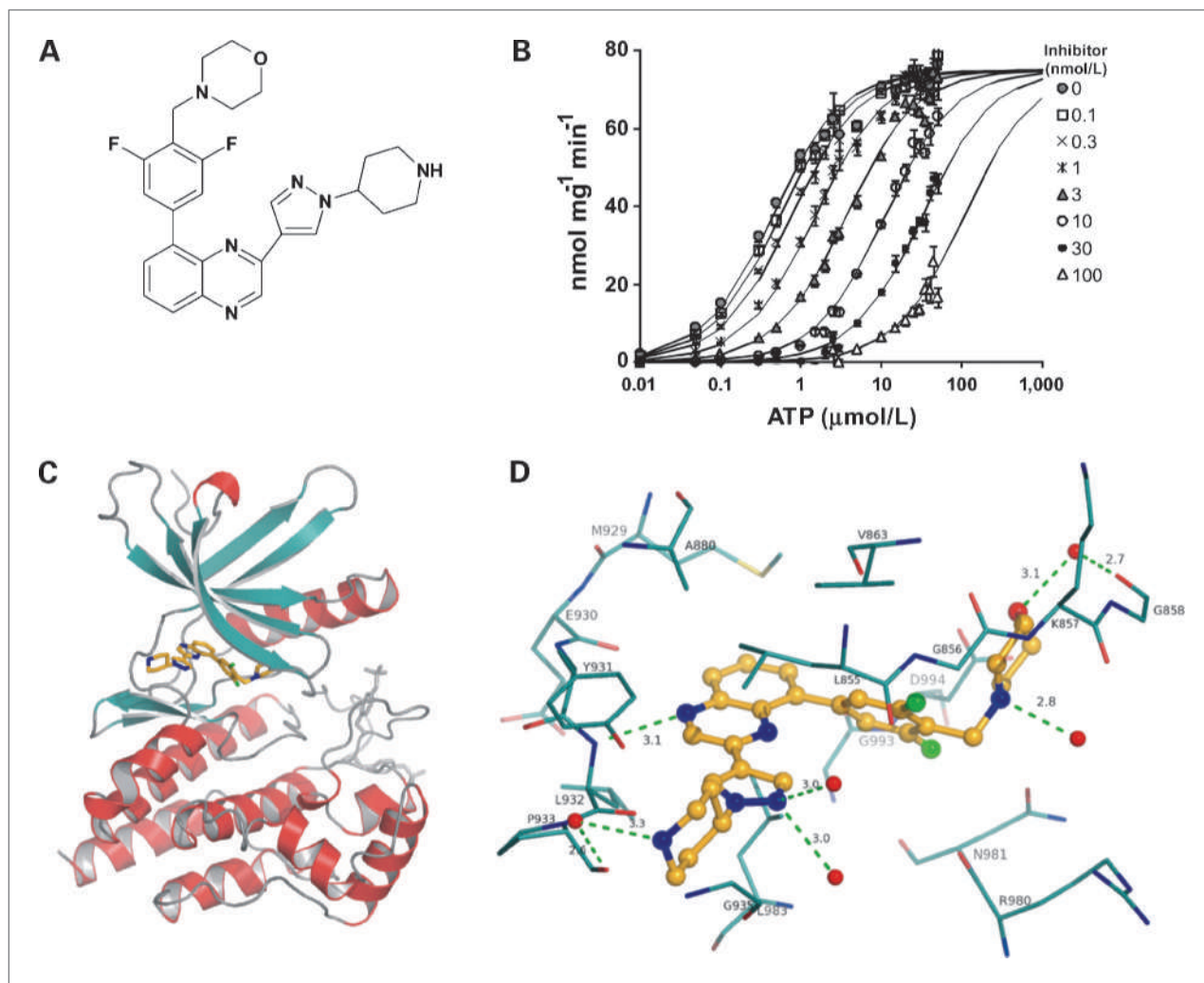


Figure 1. Inhibition of JAK2 catalytic activity by a novel ATP-competitive substituted quinoxaline. **A**, structure of NVP-BSK805. **B**, the binding mode of NVP-BSK805 was studied using the JAK2 JH1 domain enzyme. Points, mean specific activities from three experiments, each with duplicate plates. Curves were fitted to a competition model by nonlinear three-dimensional regression. NVP-BSK805 concentrations (nmol/L) are indicated in the graph. **C**, overall ribbon representation of the kinase domain with the bound inhibitor shown as stick model. **D**, close-up of NVP-BSK805 binding to the JAK2 kinase domain. Polar contacts between the protein, the inhibitor molecule, and solvent are indicated by dotted green lines.

NVP-BSK805 blocks the growth of JAK2^{V617F} cells and induces apoptosis

Next, NVP-BSK805 was tested for its ability to modulate cell proliferation. To this end, we used Ba/F3 cell-based assays of JAK2^{V617F} dependency (22, 23) and a panel of JAK2^{V617F}-bearing acute myeloid leukemia cell lines derived from patients with a history of cMPNs (24). In proliferation assays with most of these cellular models, NVP-BSK805 exhibited half-maximal growth inhibition (GI_{50}) at concentrations <100 nmol/L (Table 2). As counter-screens, we used BCR-ABL mutant K-562 and JAK3^{A572V}-mutant CMK cells and we also profiled the pan-JAK inhibitor "JAK inhibitor 1" in these assays for sake of comparison. In K-562 cells, NVP-BSK805 suppressed growth with a GI_{50} value of ~1.5 μ mol/L. Together with some degree of activity seen as well in the

ABL biochemical assays (Supplementary Table S1), the results imply that NVP-BSK805 elicits modest off-target inhibition of BCR-ABL. Indeed, the degree of this off-target activity should be put into perspective with data obtained using BCR-ABL inhibitors; imatinib and nilotinib were found to suppress the growth of K-562 cells with GI_{50} values in the range of 100 and 2 nmol/L, respectively (data not shown). In CMK cells, the GI_{50} value of NVP-BSK805 was in the range of 2 μ mol/L, seemingly consistent with the JAK family selectivity observed in biochemical assays. JAK inhibitor 1 suppressed the growth of CMK cells with a GI_{50} value in the range of 400 nmol/L, in agreement with a previous report (25), whereas antiproliferative activity in SET-2 cells was similar to NVP-BSK805 (Table 2). Interestingly, both drugs also displayed potent inhibition of two FLT3-ITD mutant cell lines (Table 2).

Table 1. Activity of NVP-BSK805 assessed in JAK radiometric filter binding kinase assays and compared with JAK inhibitor 1

	NVP-BSK805, IC ₅₀ (nmol/L) ± SE	JAK inhibitor 1, IC ₅₀ (nmol/L) ± SE
JAK1 JH1	31.63 ± 1.36	3.21 ± 0.27
JAK2 JH1	0.48 ± 0.02	1.04 ± 0.04
JAK3 JH1	18.68 ± 0.94	2.08 ± 0.09
TYK2 JH1	10.76 ± 0.89	1.56 ± 0.08
FL JAK2 V617F	0.56 ± 0.04	1.73 ± 0.05
FL JAK2 wt	0.58 ± 0.03	1.59 ± 0.09

NOTE: Half-maximal inhibitory concentrations ± SE were obtained by global fitting of the data of two independent experiments to the logistic equation (nonlinear regression).

Abbreviations: JH1, JAK homology 1; FL, full-length; wt, wild-type.

To further corroborate JAK2 selectivity of NVP-BSK805 within the JAK family, we determined concentration-dependent suppression of constitutive STAT5 phosphorylation in SET-2 and MB-02 cells as compared with CMK cells. Depletion of individual JAK family members by RNAi confirmed the dependency of constitutive STAT5 phosphorylation on JAK2 in the JAK2^{V617F}-bearing SET-2 and MB-02 cells (Fig. 2A), whereas JAK1 and JAK3, but not JAK2, were required in JAK3^{A572V}-mutant CMK cells (Fig. 2B). In the JAK2^{V617F}-mutant cell lines, NVP-BSK805 was found to potently suppress STAT5 phosphorylation at ≥100 nmol/L concentrations (Fig. 2C and D). In contrast, NVP-BSK805 concentrations exceeding 1 μmol/L were needed to blunt STAT5 phosphorylation in CMK cells (Fig. 2D). Incubation of SET-2 cells with 150 nmol/L and 1 μmol/L of NVP-BSK805, which corresponds to concentrations yielding 75% and 95% growth

inhibition, respectively, for 24, 48, and 72 hours lead to concentration- and time-dependent induction of apoptosis, as evidenced by the detection of cleaved PARP, reduced Bcl-xL expression (Fig. 3A), and a strong increase in the number of cells with less than 2N DNA content (Fig. 3B and C). Similar effects have recently been reported in SET-2 cells treated with a structurally distinct JAK2 inhibitor (26).

NVP-BSK805 suppresses JAK2^{V617F}-driven leukemic disease *in vivo*

Plasma pharmacokinetics of NVP-BSK805 was determined in rodents. In mice, the elimination half-life was 5.5 hours, clearance was 22 mL/min/kg, and volume of distribution was 5.9 L/kg. Absolute oral bioavailability was estimated to be 45% (Supplementary Fig. S1A and C). In rats, NVP-BSK805 had a terminal half-life of 18 hours, was cleared with 23 mL/min/kg,

Table 2. Activity of NVP-BSK805 in cellular assays

Cellular assay	NVP-BSK805, GI ₅₀ , IC ₅₀ (μmol/L)	JAK inhibitor 1, GI ₅₀ (μmol/L)
Ba/F3 JAK2 ^{V617F} proliferation assay	0.039 ± 0.023	ND
SET-2 JAK2 ^{V617F} proliferation assay	0.051 ± 0.018	0.070 ± 0.017
MB-02 JAK2 ^{V617F} proliferation assay	0.064 ± 0.017	0.022 ± 0.003
UKE-1 JAK2 ^{V617F} proliferation assay	0.071 ± 0.002	0.104 ± 0.013
MUTZ-8 JAK2 ^{V617F} proliferation assay	0.331 ± 0.090	0.227 ± 0.047
SET-2 JAK2 ^{V617F} P-STAT5 Surefire AlphaScreen	0.140 ± 0.046	ND
HT1080 STAT1-GFP nuclear translocation assay	0.267 ± 0.015	0.180 ± 0.066
MOLM-13 FLT3-ITD proliferation assay	0.309 ± 0.023	0.300 ± 0.060
MV4;11 FLT3-ITD proliferation assay	0.062 ± 0.022	0.333 ± 0.172
CMK JAK3 ^{A572V} proliferation assay	2.160 ± 0.167	0.431 ± 0.046
K-562 BCR-ABL proliferation assay	1.471 ± 0.081	>10

NOTE: Where indicated, the pan-JAK inhibitor “JAK inhibitor 1” was assessed for the sake of reference. GI₅₀ (proliferation assays) and IC₅₀ (AlphaScreen and Cellomics NucTrans assay) values represent means of at least two independent experiments ± SD. Abbreviation: ND, not determined.

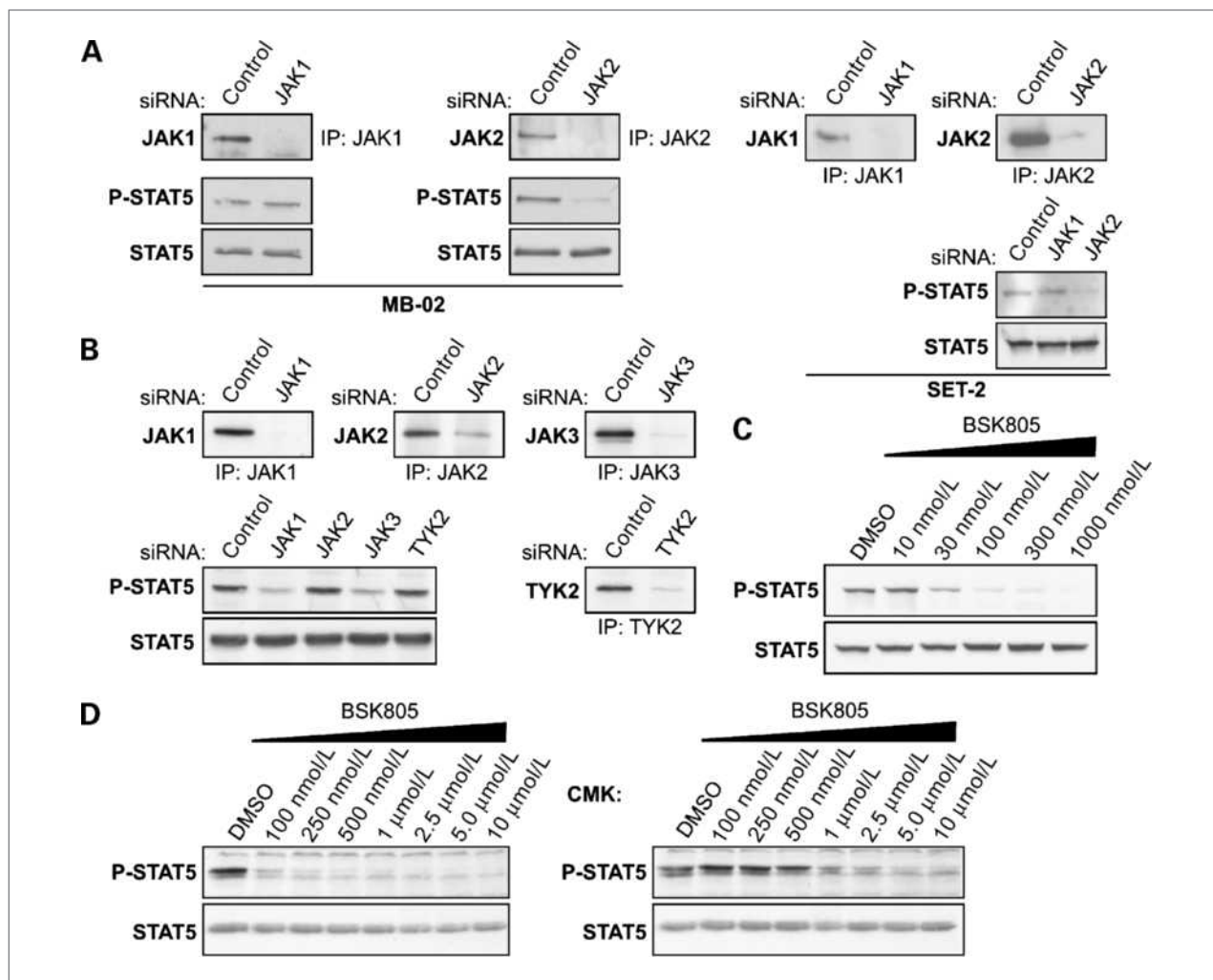


Figure 2. NVP-BSK805 potently suppresses STAT5 phosphorylation in JAK2^{V617F} mutant cell lines and displays a bias for JAK2 over JAK1 and JAK3 inhibition. **A**, JAK1 or JAK2 were depleted in JAK2^{V617F} mutant MB-02 and SET-2 cells by RNAi followed by Western blotting to detect levels of STAT5 phosphorylation. Controls were treated with nontargeting siRNA oligos. The degree of JAK knockdown was verified by immunoprecipitation and Western blotting. **B**, JAK family members were depleted in JAK3^{A572V} mutant CMK cells by RNAi. Levels of STAT5 phosphorylation and the degree of JAK knockdown were assessed as described above. **C**, MB-02 cells were treated with increasing concentrations of NVP-BSK805 for 30 min and levels of phosphorylated STAT5 were determined as described above. **D**, SET-2 cells and CMK cells were treated with increasing concentrations of NVP-BSK805 for 1 h. Levels of phosphorylated STAT5 and total STAT5 were determined by Western blotting.

and distributed extensively to tissues with a volume of distribution of 33 L/kg (Supplementary Fig. S1B and C). Oral bioavailability in rats was 50%, comparable with bioavailability in mice.

The activity of NVP-BSK805 *in vivo* was evaluated using two mouse mechanistic models. The first model was based on Ba/F3 cells stably transfected with human EpoR and JAK2^{V617F} (23), whereas the second model took advantage of the fact that subcutaneous injection of recombinant human erythropoietin (rhEpo) induced transient polycythemia and splenomegaly in rodents (27, 28). In the first model, JAK2^{V617F}-dependent Ba/F3 cells (2) were injected i.v. into the tail vein of SCID beige mice, giving rise to leukemic disease with splenomegaly (Supplementary Fig. S2). To test the ability of NVP-BSK805 to

modulate JAK2^{V617F}/STAT5 signaling in the spleen, mice were given 150 mg/kg orally of NVP-BSK805 on day 9 post-Ba/F3 cell injection, when most of the spleen consisted of Ba/F3 cells. NVP-BSK805 was found to cause prolonged suppression of STAT5 phosphorylation in spleen extracts, reducing levels by nearly half relative to vehicle-treated controls at the 6- and 12-hour time points (Fig. 4A). Measurement of compound levels in the blood by liquid chromatography/tandem mass spectrometry revealed sustained exposure of 2.8 ± 0.7 , 2.5 ± 0.3 , and 3.2 ± 0.8 μmol/L (mean \pm SEM) at the 2-, 6-, and 12-hour time points, respectively, consistent with the pharmacokinetic properties (Supplementary Fig. S1). In a subsequent experiment, mice bearing Ba/F3 cells received either vehicle or 150 mg/kg of NVP-BSK805 and

spleens were sampled after 12 hours for the detection of STAT5 phosphorylation by immunohistochemistry. In vehicle control animals, cells staining positive for STAT5 phosphorylation with varying intensities were seen throughout the spleen section and staining was confined to the area of the nucleus, which was suppressed in spleen sections of NVP-BSK805-treated animals (Fig. 4B, insets). To assess the ability of the compound to control JAK2^{V617F}-dependent leukemic disease, oral daily dosing of NVP-BSK805 at 50 or 150 mg/kg was initiated on day 5 post-Ba/F3 cell injection, 1 day after leukemic burden was evident following bioluminescence measurements. On day 9, whole-body bioluminescence readings indicated that compound-treated mice had a

significantly lower leukemic load as compared with the vehicle control group (Fig. 4C). Body weight loss was not evident in any of the treatment groups, indicating that the dosing regimens were well tolerated. Upon necropsy on day 9, it was found that NVP-BSK805 elicited a dose-dependent suppression of splenomegaly, and spleen weights in the 150 mg/kg daily dosing group were in the range considered normal for SCID beige mice (Fig. 4D).

NVP-BSK805 controls rhEpo-induced extramedullary erythropoiesis and polycythemia *in vivo*

It has been shown that treatment of rodents with rhEpo elevates reticulocyte count, hematocrit and

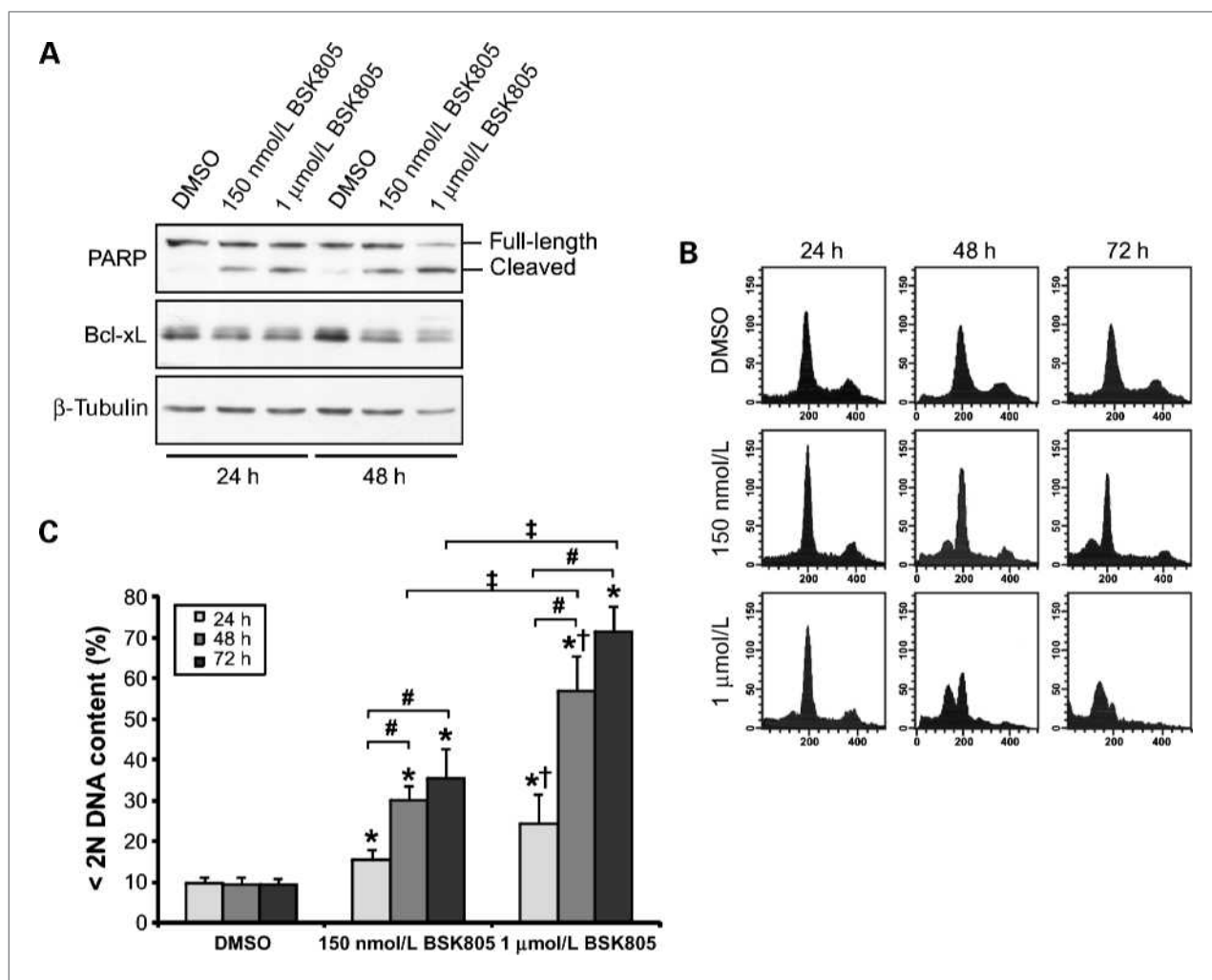


Figure 3. NVP-BSK805 induces apoptosis in JAK2^{V617F}-mutant SET-2 cells in a dose- and time-dependent manner. **A**, JAK2^{V617F} mutant SET-2 cells were treated with DMSO, 150 nmol/L of NVP-BSK805, or 1 μmol/L of NVP-BSK805 for 24 and 48 h. PARP cleavage as well as Bcl-xL levels were assessed by Western blotting. β-Tubulin was probed as a loading control. **B**, DNA content in SET-2 cells was measured by fluorescence-activated cell sorting using propidium iodide staining following treatment of cells with DMSO, 150 nmol/L of NVP-BSK805, or 1 μmol/L of NVP-BSK805 for 24, 48, and 72 h. The X and Y-axes represent FL2-A fluorescence intensity for propidium iodide staining and cell count, respectively. Results depict a representative experiment. **C**, percentage of cells with <2N DNA content at each dose and time point (columns, mean of four independent experiments; bars, SD). *, significantly different from DMSO control at respective time points using *t* test or, if not applicable, †Mann-Whitney rank sum test (*P* < 0.05). Significant difference between time points (#) or doses (‡) as assessed by *t* test (*P* < 0.05).

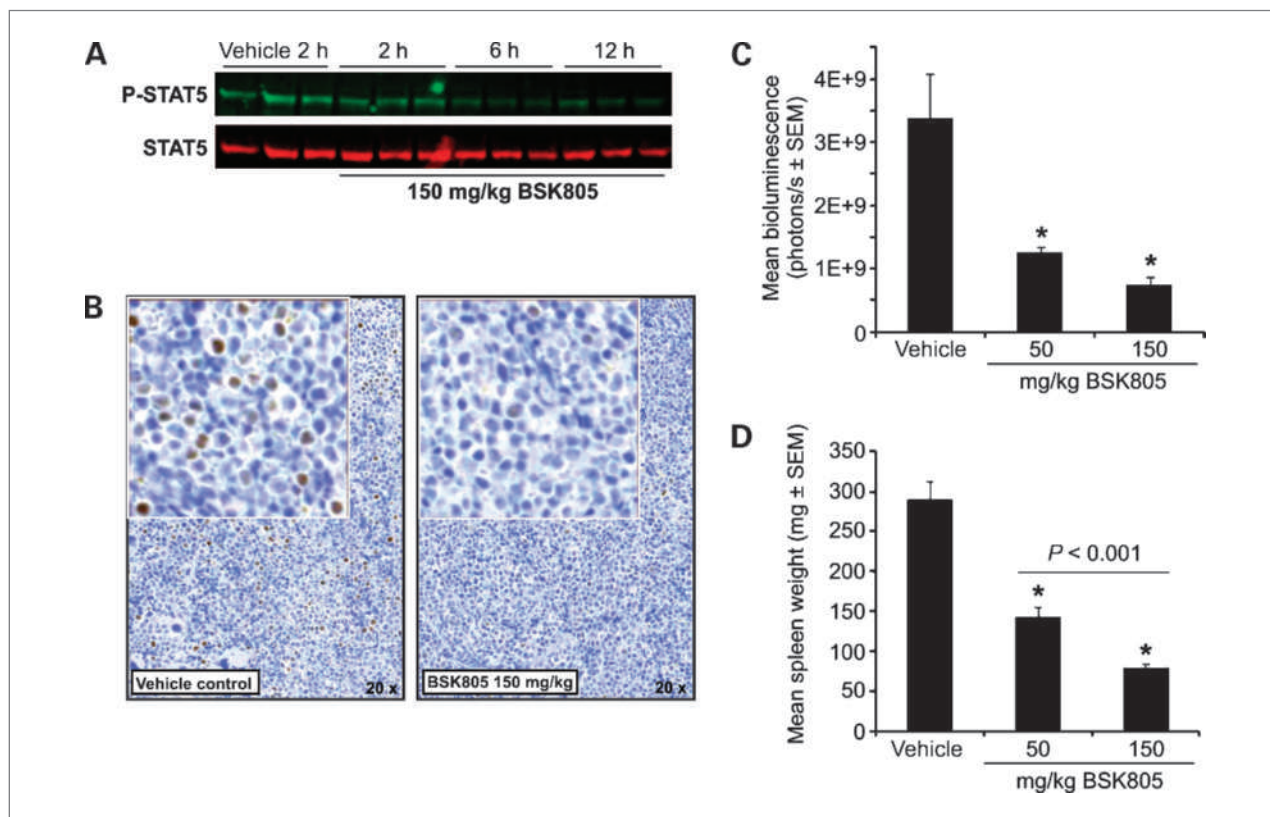


Figure 4. NVP-BSK805 suppresses STAT5 phosphorylation, splenomegaly, and leukemic cell spreading in a Ba/F3 JAK2^{V617F} cell-driven mouse model. **A**, SCID beige mice (bearing Ba/F3 JAK2^{V617F} cells) were given 150 mg/kg NVP-BSK805 orally or vehicle and sacrificed after 2, 6, and 12 h. Spleens were extracted for detection of phosphorylated STAT5 and total STAT5 levels by quantitative Western blotting. **B**, in SCID beige mice bearing Ba/F3 JAK2^{V617F} cells, STAT5 phosphorylation was readily detectable throughout the spleen sections by immunohistochemistry. Inset, the phosphorylated STAT5 staining is predominantly nuclear. Phosphorylated STAT5 is strongly reduced in mice that were given 150 mg/kg NVP-BSK805 orally after 12 h. **C**, Ba/F3 JAK2^{V617F} cell leukemic burden was detected on day 4 post-cell injection by measuring bioluminescence *in vivo* (mean, $3.8 \times 10^7 \pm 5.0 \times 10^6$ photons/s \pm SEM), and mice were randomized into treatment groups of 9 to 10 animals. Treatment was initiated with vehicle or with 50 and 150 mg/kg of NVP-BSK805 on day 5. Whole body bioluminescence reading on day 9 reveals suppression of leukemic cell spreading: 36% and 22% T/C were achieved with 50 and 150 mg/kg of NVP-BSK805, respectively (*, $P < 0.05$ versus vehicle treated animals; one-way ANOVA followed by post hoc test Dunnett's using log₁₀ transformed values). **D**, assessment of spleen weight at the time of necropsy in the frame of the efficacy experiment outlined above showed dose-dependent suppression of splenomegaly by NVP-BSK805 (*, $P < 0.05$ versus vehicle-treated animals; one-way ANOVA followed by post hoc test Dunnett or Tukey for multiple comparison using log₁₀ transformed values). Note that the spleen weight in naïve SCID beige mice is in the range of 50 mg.

erythropoiesis in the spleen, and that the latter process induces splenomegaly (29–31). rhEpo administration protocols were adapted in mice (Supplementary Fig. S3) and rats to assess the modulation of rhEpo-induced erythropoiesis stemming from the stimulation of erythroid progenitors in the bone marrow and spleen (32), which are considered target tissues in PV, by candidate JAK2 inhibitors. Using quantitative Western blotting, it was determined that rhEpo induced a 3.6-fold increase of STAT5 phosphorylation in spleen extracts over baseline 3 hours after s.c. injection (Fig. 5A). Concomitant treatment with NVP-BSK805 suppressed rhEpo-induced STAT5 phosphorylation in spleen in a dose-dependent manner, with only 2.4-, 1.6-, and 1.2-fold increases of rhEpo-induced STAT5 phosphorylation in spleen extracts over baseline upon dosing 25, 50, and 100 mg/kg, respectively (Fig. 5A). Next, mice were given daily s.c. injections of 10 units

of rhEpo for 4 consecutive days along with once daily oral administration of NVP-BSK805 dosed at 50, 75, and 100 mg/kg. Control groups received either saline injections instead of rhEpo along with oral administration of the drug vehicle, rhEpo/vehicle, or NVP-BSK805 dosed at 100 mg/kg. All animals were sacrificed on day 5. Upon necropsy, spleen weights in the rhEpo control group increased by more than 2-fold, whereas NVP-BSK805 treatment was found to suppress rhEpo-induced splenomegaly, with the 100 mg/kg dose essentially normalizing spleen weights (Fig. 5B). The same drug dose administered without rhEpo injections showed a trend to suppress spleen weights below the baseline. NVP-BSK805 also suppressed rhEpo-induced increases in reticulocyte count and hematocrit in blood (Fig. 5C and D), as well as erythroblast expansion in the spleen and bone marrow (Supplementary Fig. S4A and B). The other hematologic variables were not significantly altered

(data not shown), except for an increase in platelet count in animals that were given the JAK2 inhibitor (Supplementary Fig. S4C).

Similarly, NVP-BSK805 suppressed rhEpo-induced splenomegaly and polycythemia in rats. Rats were given daily s.c. injections of 25 units of rhEpo for 14 consecutive days along with once daily oral administration of NVP-BSK805 dosed at 12.5, 25, and 50 mg/kg. Control groups received either saline injections instead of rhEpo along with oral administration of the drug vehicle or rhEpo/vehicle. Near normalization of rhEpo-induced splenomegaly was seen with the 25 mg/kg/d dose, whereas 50 mg/kg/d entirely prevented splenomegaly (Supplementary Fig. S5A). Furthermore, NVP-BSK805 administration resulted in a trend for dose-dependent suppression of rhEpo-induced increases

in reticulocyte count (Supplementary Fig. S5B) and hematocrit (data not shown) without a significant effect on other blood cell variables (data not shown), except for an increase in platelet count in compound-treated animals (Supplementary Fig. S5C). The compound was well tolerated as assessed by measuring body weight, with somewhat reduced rate of body weight gain in animals treated with the highest dose (Supplementary Fig. S5D).

Discussion

The high frequency of activating point mutations in JAK2 and MPL, specifically in cMPNs, represents a striking example of disease dependency on an aberrantly activated signal transduction pathway. Consequently, JAK2

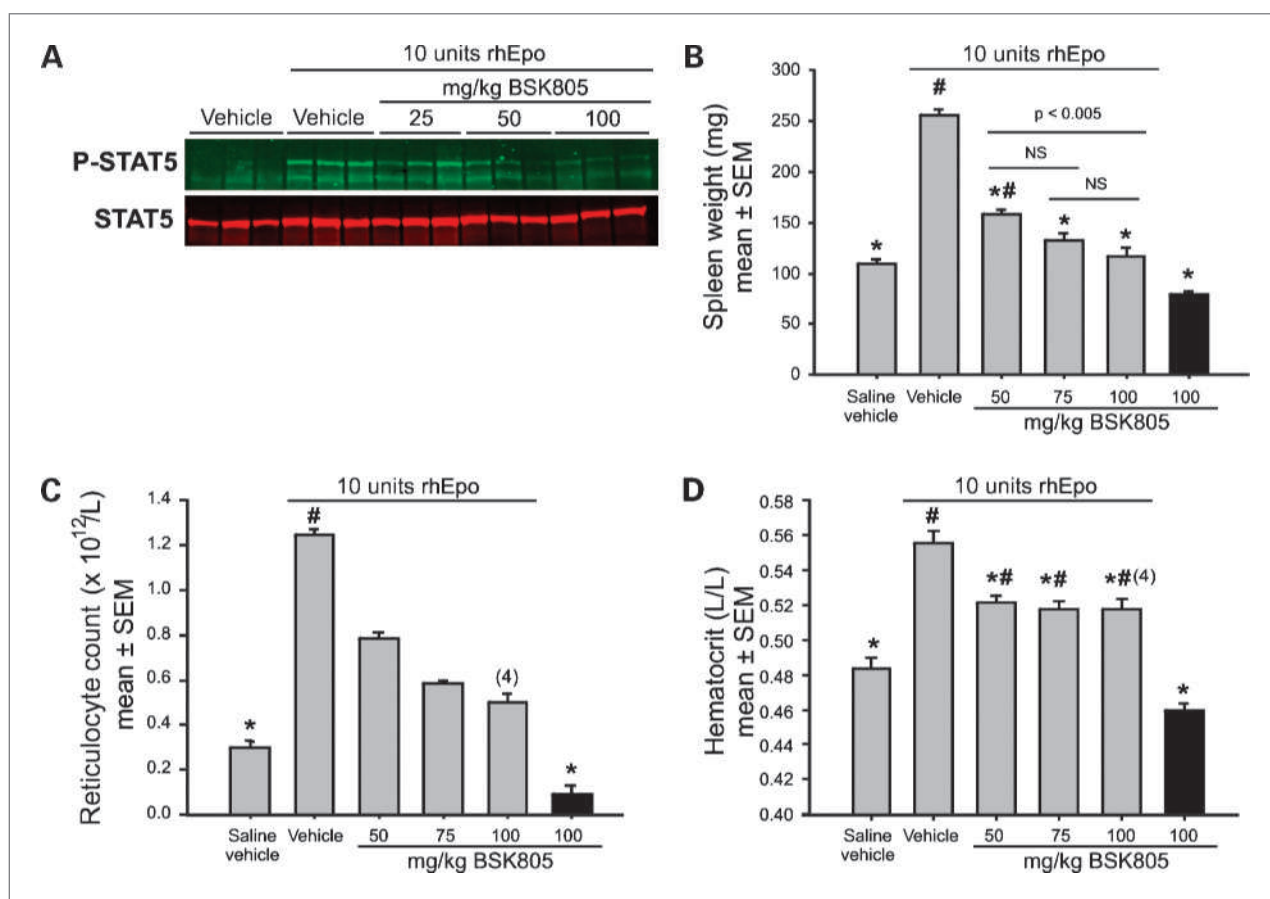


Figure 5. NVP-BSK805 suppresses rhEpo-induced STAT5 phosphorylation as well as rhEpo-mediated polycythemia and splenomegaly in BALB/c mice. **A**, mice received a s.c. injection of 10 units of rhEpo and were given 25, 50, and 100 mg/kg orally of NVP-BSK805. Control animals received either a s.c. injection of saline or 10 units of rhEpo and were given vehicle orally. Animals were sacrificed 3 h later and spleen samples were processed for detection of STAT5 phosphorylation by Western blotting. **B–D**, mice received daily injections of 10 units of rhEpo on 4 consecutive days. Concomitantly, mice were orally dosed with vehicle or with NVP-BSK805 at 50, 75, and 100 mg/kg. Controls received injections of saline and oral administration of vehicle or NVP-BSK805 dosed at 100 mg/kg (black column). $n = 5$ /group, except the group dosed with NVP-BSK805 alone ($n = 3$). Animals were sacrificed 24 h after the final treatment for analysis: histograms depict mean spleen weight (**B**), reticulocyte count (**C**) and hematocrit (**D**). Numbers in parentheses depict the number of samples per group amenable to analysis of the respective variable, if smaller than number of animals per group (e.g., flags due to clotting). *, $P < 0.05$ versus rhEpo-treated animals; #, $P < 0.05$ versus saline-treated animals (one-way ANOVA followed by post hoc Dunnett's or ANOVA on ranks followed by Dunn's test for reticulocyte count). The post hoc Tukey's test was used for intergroup comparison.

has emerged as a promising target for the treatment of cMPNs and first-generation JAK inhibitors have rapidly progressed into the clinic since the discovery of these activating mutations. Encouragingly, clinical trials with JAK2 inhibitors in patients with primary myelofibrosis have shown rapid suppression of splenomegaly and improvement of constitutional symptoms (33), clearly warranting further clinical investigation. However, the disease-modifying effects on variables such as leukocytosis, anemia, mutant allele burden, or bone marrow fibrosis have not yet met expectations (34). Additional drug discovery efforts on this challenging target as well as continued preclinical research are anticipated to yield JAK2 inhibitors with different selectivity and pharmacokinetic profiles and might open up avenues to improve therapeutic outcome.

Here, we describe the characterization of NVP-BSK805 in biochemical and cellular assays, and the assessment of its pharmacologic properties in mouse and rat models. NVP-BSK805 is a potent ATP-competitive inhibitor of V617F mutant and wild-type JAK2 enzymes with favorable selectivity factors over the other JAK family members. Importantly, NVP-BSK805 also shows a good selectivity profile over other kinases assessed, which included tyrosine and serine/threonine protein kinases as well as lipid kinases. The potent biochemical activity translated into robust suppression of JAK2 signaling in cellular systems. The pharmacokinetic properties of NVP-BSK805 in mouse and rat are characterized by low to intermediate clearance, with a high volume of distribution and a long elimination half-life. Oral bioavailability is in the range of 50%. Pharmacodynamic evaluation in mouse models revealed suppression of JAK2-mediated STAT5 phosphorylation in the spleen at doses of 100 mg/kg and above. Importantly, doses of NVP-BSK805 that modulated the molecular pharmacodynamic marker also resulted in efficacy in these models upon daily dosing, while being well tolerated. Thus, although NVP-BSK805 is not a candidate for clinical development due to photostability, it represents a potent, selective, and *in vivo* efficacious JAK2 inhibitor tool compound for preclinical research.

In mouse and rat models of rhEpo-mediated polycythemia, the compound displayed selective effects on the erythroid lineage, suppressing increases in reticulocyte count and splenomegaly, which is consistent with its mode of action and JAK family selectivity. As this article was being prepared, Mathur and colleagues reported similar results in their mouse polycythemia model with a pyridone containing tetracyclic JAK inhibitor (35), indicating that chronic therapy with JAK2 inhibitors might be useful in controlling RBC count and extramedullary hematopoiesis in patients suffering from PV. Of note, in both mice and rats, NVP-BSK805 treatment led to an elevation of platelet count beyond the upper limit of the reference interval (36). Although rhEpo administration on its own led to a slightly elevated platelet count in mice, in agreement with an earlier report (29), the increase in platelet count was

also seen in animals that were given the JAK2 inhibitor without receiving rhEpo injections. One could speculate that suppression of the erythroid lineage by a JAK2 inhibitor might favor the expansion of megakaryocytes according to models of stem cell competition between erythroid and megakaryocytic precursors (37). However, as for Epo/EpoR signaling, TPO/MPL signal transduction also relies on JAK2 to a large degree (38). Further studies with JAK2 inhibitors will be needed to elucidate the mechanism underlying this phenomenon and to be able to judge if particular caution in the treatment of patients with PV or essential thrombocythemia with high baseline platelet count using certain inhibitors is indicated. To this end, testing of JAK2 inhibitors in animal models that exhibit thrombocytosis will be important, e.g., models of MPL^{W515L}-mediated myelofibrosis with megakaryocytic proliferation (10) or JAK2^{V617F}-driven essential thrombocythemia-like phenotypes (39).

A key question that arose from clinical trials in primary myelofibrosis with first-generation JAK inhibitors is how disease modification could be improved. All current JAK2 inhibitors, including NVP-BSK805, target not only the mutated enzyme but also wild-type JAK2 due to their ATP-competitive mode of action. Obviously, for cMPN therapy, inhibitors that only target signaling stemming from mutant JAK2 would be ideal, e.g., a hypothetical small molecule drug that exclusively interacts with the mutated pseudokinase domain to restore its inhibitory function (40). However, this approach represents a formidable challenge from the drug discovery point of view. Notwithstanding these challenges, there might be options to improve the therapeutic outcomes of existing JAK inhibitors by combining them with other targeted therapies. Such combinations would aim at attacking the mutated clone from different angles, e.g., by suppressing JAK2 signaling and survival signals emanating from the hematopoiesis-inducing microenvironment. Besides cytokine and growth factor signals, events such as loss of the TET2 tumor suppressor (41) might cooperate with aberrant JAK2 signaling in disease progression. Gaining a better understanding of the altered signaling that supports the expansion and survival of the mutant clone will provide a rationale for JAK2 inhibitor combinations. In this context, NVP-BSK805 represents a suitable tool compound to explore combinations of JAK2 inhibitors with other agents in preclinical models of myeloproliferative-like diseases and other hematologic malignancies to identify modalities that may be worthwhile exploring for disease-modification in the clinical setting.

Disclosure of Potential Conflicts of Interest

All authors are or have been full-time employees of Novartis Pharma AG.

Acknowledgments

The authors thank Prof. Michael Eck for providing the JAK2 construct for the X-ray crystallography and enzymatic studies;

Dr. Ross Levine for critical reading of the manuscript and fruitful discussion; Profs. Doris Morgan, Hans Drexler, and Walter Fiedler for the generous gift of cell lines; Dr. Gang Xia for providing Ba/F3 cells stably expressing EpoR, JAK2^{V617F}, and luciferase; and finally, the authors thank Joëlle Rubert, Zhiyao Qian, Rita Andraos, Fanny Marque, Caroline Fux, Violetta Powajbo, and Francesca Santacroce for their excellent technical assistance.

The costs of publication of this article were defrayed in part by the payment of page charges. This article must therefore be hereby marked *advertisement* in accordance with 18 U.S.C. Section 1734 solely to indicate this fact.

Received 01/20/2010; revised 04/16/2010; accepted 05/10/2010; published OnlineFirst 06/29/2010.

References

- James C, Ugo V, Le Couedic J-P, et al. A unique clonal JAK2 mutation leading to constitutive signalling causes polycythaemia vera. *Nature* 2005;434:1144–8.
- Levine RL, Wadleigh M, Cools J, et al. Activating mutation in the tyrosine kinase JAK2 in polycythemia vera, essential thrombocythemia, and myeloid metaplasia with myelofibrosis. *Cancer Cell* 2005; 7:387–97.
- Kralovics R, Passamonti F, Buser AS, et al. A gain-of-function mutation of JAK2 in myeloproliferative disorders. *N Engl J Med* 2005;352: 1779–90.
- Thompson JE. JAK protein kinase inhibitors. *Drug News Perspect* 2005;18:305–10.
- Mesa RA. Navigating the evolving paradigms in the diagnosis and treatment of myeloproliferative disorders. *Hematology* 2007;2007: 355–62.
- Tefferi A, Gilliland DG. JAK2 in myeloproliferative disorders is not just another kinase. *Cell Cycle* 2005;4:4053–6.
- Scott LM, Tong W, Levine RL, et al. JAK2 exon 12 mutations in polycythemia vera and idiopathic erythrocytosis. *N Engl J Med* 2007;356: 459–68.
- Bercovich D, Ganmore I, Scott LM, et al. Mutations of JAK2 in acute lymphoblastic leukaemias associated with Down's syndrome. *Lancet* 2008;372:1484–92.
- Kearney L, Gonzalez De Castro D, Yeung J, et al. Specific JAK2 mutation (JAK2R083) and multiple gene deletions in Down syndrome acute lymphoblastic leukemia. *Blood* 2009;113:646–8.
- Pikman Y, Lee BH, Mercher T, et al. MPLW515L is a novel somatic activating mutation in myelofibrosis with myeloid metaplasia. *PLoS Med* 2006;3:e270.
- Pardanani AD, Levine RL, Lasho T, et al. MPL515 mutations in myeloproliferative and other myeloid disorders: a study of 1182 patients. *Blood* 2006;108:3472–6.
- Weniger MA, Melzner I, Menz CK, et al. Mutations of the tumor suppressor gene SOCS-1 in classical Hodgkin lymphoma are frequent and associated with nuclear phospho-STAT5 accumulation. *Oncogene* 2006;25:2679–84.
- Lacronique V, Boureux A, Della Valle V, et al. A TEL-JAK2 fusion protein with constitutive kinase activity in human leukemia. *Science* 1997;278:1309–12.
- Verstovsek S. Therapeutic potential of Janus-activated kinase-2 inhibitors for the management of myelofibrosis. *Clin Cancer Res* 2010; 16:1988–96.
- Pissot-Soldermann C, Gerspacher M, Furet P, et al. Discovery and SAR of potent, orally available 2,8-diaryl-quinoxalines as a new class of JAK2 inhibitors. *Bioorg Med Chem Lett* 2010;20: 2609–13.
- Lucet IS, Fantino E, Styles M, et al. The structural basis of Janus kinase 2 inhibition by a potent and specific pan-Janus kinase inhibitor. *Blood* 2006;107:176–83.
- Shannon K, Van Etten RA. JAKing up hematopoietic proliferation. *Cancer Cell* 2005;7:291–3.
- Stepkowski SM, Kirken RA. Janus tyrosine kinases and signal transducers and activators of transcription regulate critical functions of T cells in allograft rejection and transplantation tolerance. *Transplantation* 2006;82:295–303.
- Levine RL, Pardanani A, Tefferi A, Gilliland DG. Role of JAK2 in the pathogenesis and therapy of myeloproliferative disorders. *Nat Rev Cancer* 2007;7:673–83.
- Erdmann D, Allard B, Bohn J, et al. Kinetic study of human full-length wild-type JAK2 and V617F mutant proteins. *Open Enzyme Inhib J* 2008;1:80–4.
- Thompson JE, Cubbon RM, Cummings RT, et al. Photochemical preparation of a pyridone containing tetracycline: a Jak protein kinase inhibitor. *Bioorg Med Chem Lett* 2002;12:1219–23.
- Lu X, Levine R, Tong W, et al. Expression of a homodimeric type I cytokine receptor is required for JAK2V617F-mediated transformation. *Proc Natl Acad Sci U S A* 2005;102:18962–7.
- Pardanani A, Hood J, Lasho T, et al. TG101209, a small molecule JAK2-selective kinase inhibitor potentially inhibits myeloproliferative disorder-associated JAK2V617F and MPLW515L//K mutations. *Leukemia* 2007;21:1658–68.
- Quentmeier H, MacLeod RAF, Zaborski M, Drexler HG. JAK2 V617F tyrosine kinase mutation in cell lines derived from myeloproliferative disorders. *Leukemia* 2006;20:471–6.
- Walters DK, Mercher T, Gu T-L, et al. Activating alleles of JAK3 in acute megakaryoblastic leukemia. *Cancer Cell* 2006;10:65–75.
- Gozgit JM, Beberitz G, Patil P, et al. Effects of the JAK2 inhibitor, AZ960, on Pim/BAD/BCL-xL survival signaling in the human JAK2 V617F cell line SET-2. *J Biol Chem* 2008;283:32334–43.
- Muntzel M, Hannedouche T, Lacour B, Druke T. Effect of erythropoietin on hematocrit and blood pressure in normotensive and hypertensive rats. *J Am Soc Nephrol* 1992;3:182–7.
- Woo S, Krzyzanski W, Jusko WJ. Pharmacokinetic and pharmacodynamic modeling of recombinant human erythropoietin after intravenous and subcutaneous administration in rats. *J Pharmacol Exp Ther* 2006;319:1297–306.
- Shikama Y, Ishibashi T, Kimura H, Kawaguchi M, Uchida T, Maruyama Y. Transient effect of erythropoietin on thrombocytopoiesis *in vivo* in mice. *Exp Hematol* 1992;20:216–22.
- Loo M, Beguin Y. The effect of recombinant human erythropoietin on platelet counts is strongly modulated by the adequacy of iron supply. *Blood* 1999;93:3286–93.
- Vannucchi AM, Bianchi L, Cellai C, et al. Accentuated response to phenylhydrazine and erythropoietin in mice genetically impaired for their GATA-1 expression (GATA-1low mice). *Blood* 2001;97:3040–50.
- Richmond TD, Chohan M, Barber DL. Turning cells red: signal transduction mediated by erythropoietin. *Trends Cell Biol* 2005;15:146–55.
- Vannucchi AM. How do JAK2-inhibitors work in myelofibrosis: an alternative hypothesis. *Leuk Res* 2009;33:1581–3.
- Mesa R, Gale RP. Hypothesis: how do JAK2-inhibitors work in myelofibrosis. *Leuk Res* 2009;33:1156–7.
- Mathur A, Mo J-R, Kraus M, et al. An inhibitor of Janus kinase 2 prevents polycythemia in mice. *Biochem Pharmacol* 2009;78:382–9.
- Liberati T, Sansone S, Feuston M. Hematology and clinical chemistry values in pregnant Wistar Hannover rats compared with nonmated controls. *Vet Clin Pathol* 2004;33:68–73.
- McDonald T, Sullivan P. Megakaryocytic and erythrocytic cell lines share a common precursor cell. *Exp Hematol* 1993;21:1316–20.
- Parganas E, Wang D, Stravopodis D, et al. Jak2 is essential for signaling through a variety of cytokine receptors. *Cell* 1998;93:385–95.
- Tiedt R, Hao-Shen H, Sobas MA, et al. Ratio of mutant JAK2-617F to wild-type Jak2 determines the MPD phenotypes in transgenic mice. *Blood* 2008;111:3931–40.
- Saharinen P, Vihinen M, Silvennoinen O. Autoinhibition of Jak2 tyrosine kinase is dependent on specific regions in its pseudokinase domain. *Mol Biol Cell* 2003;14:1448–59.
- Delhommeau F, Dupont S, Valle VD, et al. Mutation in TET2 in myeloid cancers. *N Engl J Med* 2009;360:2289–301.

Molecular Cancer Therapeutics

Potent and Selective Inhibition of Polycythemia by the Quinoxaline JAK2 Inhibitor NVP-BSK805

Fabienne Baffert, Catherine H. Régnier, Alain De Pover, et al.

Mol Cancer Ther 2010;9:1945-1955. Published OnlineFirst June 29, 2010.

Updated version	Access the most recent version of this article at: doi: 10.1158/1535-7163.MCT-10-0053
Supplementary Material	Access the most recent supplemental material at: http://mct.aacrjournals.org/content/suppl/2010/06/28/1535-7163.MCT-10-0053.DC1

Cited articles	This article cites 41 articles, 13 of which you can access for free at: http://mct.aacrjournals.org/content/9/7/1945.full#ref-list-1
Citing articles	This article has been cited by 13 HighWire-hosted articles. Access the articles at: http://mct.aacrjournals.org/content/9/7/1945.full#related-urls

E-mail alerts	Sign up to receive free email-alerts related to this article or journal.
Reprints and Subscriptions	To order reprints of this article or to subscribe to the journal, contact the AACR Publications Department at pubs@aacr.org .
Permissions	To request permission to re-use all or part of this article, use this link http://mct.aacrjournals.org/content/9/7/1945 . Click on "Request Permissions" which will take you to the Copyright Clearance Center's (CCC) Rightslink site.